

Actual Traffic Based Load-Aware Dynamic Point Selection for LTE-Advanced System

Kittipong Nuanyai, Soamsiri Chantaraskul*

The Sirindhorn International Thai-German Graduate School of Engineering, King Mongkut's University of Technology North Bangkok, Bangkok, 10800, Thailand

ARTICLE INFO

Article history:

Received: 15 January, 2021

Accepted: 08 March, 2021

Online: 31 March, 2021

Keywords:

Coordinated MultiPoint
Dynamic Point Selection
Traffic Load Aware

ABSTRACT

Coordinated MultiPoint (CoMP) has been introduced for LTE-Advanced system to overcome the inter-cell interference problems and enhance the signal quality of cell-edge UEs (User Equipments). With such concept, the overall system performance should be improved considerably to support the significantly increasing amount of demand on data transmission via mobile communication that happens nowadays. Dynamic Point Selection (DPS) is one of the major CoMP techniques offering benefit through its practicality and low complexity. This work proposes the actual traffic-based load-aware DPS for LTE-Advanced system. The key important cell selection criterion employed in this work is based on the actual traffic load of the calls along with the UEs received signal indicator. The adapted Vienna downlink system level simulator has been used for the system evaluation. The video streaming traffic model was employed with the data rate of 512 kbps for the realistic use cases and four simulation scenarios including the uniformly distributed UEs case and different patterns of hotspots distribution use cases were deployed. The system performance evaluation includes the system throughput performance, the number of UEs achieving expected data rate, and eNBs' traffic load. The results show that our proposed method offers a substantial improvement over the traditional system as well as the system embedded with the existing DPS mechanisms when the traffic loads are imbalanced such as in certain hotspot cases.

1. Introduction

Mobile communication has entered the fifth generation (5G) with the expectation to support a dynamically increasing number of mobile users as well as the devices supporting IoT services such as e-health, smart metering, and Car2X communication. These mobile services are growing at a compound annual growth rate of 47% as shown in the cisco report [1]. To support such high demand on data transmission with the available radio resource, the Heterogeneous Networks (HetNets) has been deployed. The approach maintains the intended coverage and optimizes the overall system capacity, especially at high traffic demand. In HetNets, the service coverage area is located with cells of different sizes (with different maximum transmit power), referred to as macrocell, microcell, picocell, and possibly femtocells, forming different network tiers. Although, the 5G LTE-Advanced system can gain benefit from an implementation of HetNets, a mixture of cell sizes leads to the complexity in network planning. The Inter-Cell Interference (ICI) caused by the transmission of different base

stations in the collocating area will occur especially at the cell edge. Many works have investigated interference management technologies to improve cell-edge throughput. Inter-Cell Interference Coordination (ICIC) has been introduced in LTE Release 8 providing the coordination of neighboring cells in order to mitigate inter-cell interference for UEs at the cell edge. The Enhance ICIC or eICIC was launched in LTE Release 10. The two major techniques under eICIC include the Almost Blank Subframes (ABS) and the Cell Range Expansion (CRE) technique. Using CER, macrocell traffic can be offloaded to the small cells in the same area. The use of Almost Blank Subframes (ABS) results in the key contribution, which is the addition of time domain to ICIC. The signal will be transmitted from the macro-eNB in accordance with a semi-static pattern when eICIC is applied. In these blank subframes, UEs are able to receive the DL information (both for control data and user data) since they are at the cell edge that is normally in the CRE region of the small cells. The performance evaluation of the system embedded with CRE and ABS mechanism with diverse CRE and ABS configurations are investigated in [2].

*Corresponding Author: Soamsiri Chantaraskul, King Mongkut's University of Technology North Bangkok, Bangkok, Thailand, soamsiri.c@tggs.kmutnb.ac.th

The transmission of Coordinated MultiPoint (CoMP) was first mentioned in 3GPP Release 11 [3]. Its main concept is to reduce the inter-cell interference and improve the quality of signal of cell-edge UEs by implementing multi-cell cooperation. The new framework based on the multi-cell Channel State Information (CSI) feedback from the set of cells in a CoMP cluster was introduced. Many mechanisms have been proposed under the umbrella of CoMP. In [4], the integration between Joint Transmission (JT) CoMP and the Non-Orthogonal Multiple Access (NOMA) in the downlink HetNet was investigated. The JT CoMP scheme with the anisotropic path loss model was satisfied for the requirement of the fifth generation (5G) of mobile communication by the author of [5]. In [6], coordinated scheduling CoMP was analyzed in terms of the throughput with different cells. However, the Dynamic Point Selection (DPS) CoMP is the research gap of such work

In this work, the actual traffic load-aware Dynamic Point Selection (DPS) is proposed. The major benefit of the DPS mechanism in general is that it is a simpler approach in terms of practicality since UEs are being served by only one serving cell at a time. Several DPS mechanisms have been proposed previously in [7] and [8] without considering the traffic load condition of the cells. In [9]-[11], DPS mechanisms with cell load consideration were presented. However, the call load was estimated by the average value of the PF (Proportional Fairness) metrics and the current number of active UEs. Unlike the previous papers, this work proposes the actual traffic based load-aware DPS, in which the current traffic load of the cells is considered. The obtained results ascertain that overall system performance can be enhanced as well as the service quality especially in the cases of load imbalanced in the CoMP clusters.

This paper is organized as follows. Section 2 gives a review on CoMP techniques in LTE-Advanced system. This section presents previously proposed DPS approaches along with the traffic model used in the studies. In section 3, the algorithm design of our proposed actual traffic load-aware DPS is described. The simulation model and simulation scenario are defined in section 4. The simulation results are given along with the discussion in section 5. Finally, conclusions are given in section 6.

2. Coordinated MultiPoint in LTE-Advanced System

2.1. The Coordinated MultiPoint (CoMP)

According to [12][13][14], the basic principle of CoMP is to improve the spectrum efficiency by making use of the multiple transmitting and receiving antennas from multiple site locations though they may or may not belong to the same physical cell. Also, by taking the advantage of the co-channel interferences, the enhancement of effective coverage area can be achieved. Although CoMP is mainly used to enhance the cell-edge UE experience, it can be applied to improve the service quality of UEs experiencing intense signal from different eBSs/cells. CoMP can be divided into two terms which are inter-site CoMP and intra-site CoMP depending on the coordinating Transmission Point (TPs). If the coordination is executed between eNBs located at the separate geographical areas, it is the inter-site CoMP. If the coordination is executed among multiple antenna units between sectors of the same BS, it is the intra-site CoMP. Refer to the previously

proposed mechanisms, CoMP can be categorized into two types which are; a) Coordinated Scheduling/Beamforming (CoMP-CS/CB) and b) Joint Processing (CoMP-JP).

• Coordinated Scheduling/Beamforming (CS/CB)

In CS/CB CoMP, the data packet requiring to be sent to a UE terminal are ready for transmitting from only one BS in the CoMP cooperating set [15], whereas the user scheduling and beamforming decision are dynamically obtained after the coordination among all TPs in the cooperating set is completed. By applying the semi-static point selection, the transmission decision is made. Although fast and strict coordination can be obtained from CS/CB, the selection of the users' best serving set for transmitter's beams construction is still based upon their geographical position. This is because the beamforming in a coordinated manner of CS/CB relies on the capabilities of the MIMO antenna. Focusing on the behavior of the beam to resources selection, as shown in Figure 1(a), the coordinated generation of beams manages not only to obtain the interference reduction among other neighboring users, but also the enhancement of signal strength of the targeted users.

• Joint Processing (JP)

The most advanced CoMP scheme that has been commonly applied to achieve spectral efficiency improvement, especially for the cell-edge user, is the JP scheme. In this case, considering the same time-frequency resource, the UE's data is available at more than one TP in the CoMP set. In terms of cooperation mechanisms, there are two main categories of CoMP-JP including Joint Transmission CoMP (JT-CoMP) and Dynamic Point Selection CoMP (DPS-CoMP).

Joint Transmission CoMP (JT): In the JT-CoMP scheme, UE data is processed and transmitted from the multiple cooperating BSs at the same time. Even in the heterogeneous scenario and dense small cell network with low power nodes, the essential signal strength delivered from the multiple BSs can be simultaneously sensed by the UEs. Although the JT-CoMP is the most powerful and attractive approach applied to enhance the efficiency of the spectrum and the average throughput, it requires high system demand in terms of computational power and signaling overhead as presented in Figure 1(b).

Dynamic Point Selection CoMP (DPS): In the traditional DPS-CoMP scheme, UEs can reselect the serving BS by considering the highest received SINR and the minimum path loss. However, the DPS-CoMP is different from the CS CoMP in that all cooperating BSs contain the UE's data in DPS. The UE performs the selection of the best serving BS for its next frame dynamically and then notifies all cooperating BSs of the CoMP set. As shown in Figure 1(c), after the newly serving BS is chosen, it informs the others to refrain from transmission via the X2 interface. This action is done to support the resources that this UE is about to employ. Therefore, the transmission of data is taken place only by one BS at a time.

In the baseline scheme of the DPS, the transmission switching metric can be defined as.

$$S_k^{s,t} = \frac{r_k^t}{r_k^s} \quad (1)$$

where the term r_k^t is the instantaneous throughputs of user k when being served by the TP t and r_k^s is the instantaneous throughput of user k when being served by TP s . In this basic DPS mechanism, the cell load of the eNB is not taken into account for DPS switching metric.

In [10], an instantaneous load-base DPS scheme was proposed. UE's channel and cell load of the serving cell are used to achieve the transmission switching metric. In this case, the transmission switching metric can be derived from eq. (1) by including the cell load representing the eNB load state. As a result, the transmission switching metric of the load-base DPS scheme can be defined as:

$$S_k^{s,t} = \frac{\left(\frac{r_k^t}{\rho_t}\right)}{\left(\frac{r_k^s}{\rho_s}\right)} \quad (2)$$

where the terms ρ_t and ρ_c are the cell load of the transmission point t and s , respectively.

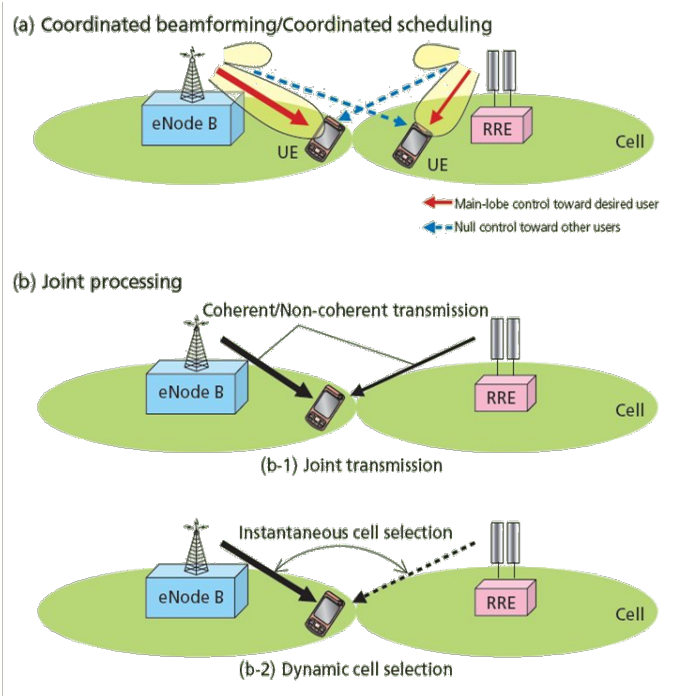


Figure 1: Downlink CoMP transmission [16]

2.2. Traffic Model Studied in DPS

The performance of DPS for LTE-Advanced system has been investigated in several works. The authors of [7] and [9] have analyzed the DPS mechanism in the homogenous networks with the full buffer traffic model. The HetNet case has been implemented in [8]. The authors of [10] and [11] have compared the performance of DPS under bursty traffic model in comparison with the full buffer traffic model. In [17], the DPS mechanism in the HetNet scenario with the FTP traffic model was implemented. Nonetheless, in such a proposed algorithm design, the bursty traffic model and the full buffer traffic modal may not be the best

type of traffic to be used. This is because when all UEs use a bursty traffic model or a full buffer traffic model, the cell is more or less need to offer full capacity, which leads to the cell load of around 100% most of the time. With that, the traffic offloading effect is hard to be monitored.

In this work, the video streaming traffic model is therefore focused, which is more or less the most used kind of services in the real world these days. The configurable video traffic model has been developed here and used to analyze the system performance embedded with our DPS with the load-aware mechanism. Table 1 presents the configurable parameters of the video streaming traffic model used in this work.

Table 1: Parameter of the video streaming traffic model

Parameters	Value
Slice size	400 bytes
Slice interarrival time (encoder delay)	6 ms
Number of slice per frame	16 slice
Data rate constraint	512 kbps
Arrival time for all slices	100 ms

3. Algorithm Design of the Proposed Actual Traffic based Load-aware DPS

3.1. Cell Load Estimation

In [7] and [8], the performance of DPS in both homogenous networks and HetNet has been analyzed. Load-aware with DPS was implemented with different mechanisms from our proposed method here. As for the cell load estimation, the authors of [9] define traffic load as the summation of the data traffic from all UEs attached with the cell. There are two approaches for cell load estimated by the author of [10] and [11]. In [10], the cell load is estimated by the average of the Proportional Fairness (PF) metrics of the UEs currently served by that cell.

$$\rho_c = \frac{\sum_{i \in \mathcal{A}_c} \frac{r_i}{x_i}}{N_c} \quad (3)$$

where ρ_c is the traffic cell load of the TP_c , \mathcal{A}_c is the set of active UEs currently served by TP_c , and $\frac{r_i}{x_i}$ is the ratio of the PF metric of UE_i . In [11], the cell load is estimated by using the current number of active UEs served by that current cell. However, in reality, traffic load of a cell cannot be estimated by the number of UEs. This is because the traffic demand of each UE is not always the same.

In this work, the actual traffic load of a cell is used for analysis in our proposed system. The actual traffic load estimation used in this work can be defined as:

$$\rho_c = \frac{\sum_{u|X(u)=c} \frac{D_u}{R(SINR_u)}}{N_{tot}} \quad (4)$$

where D_u is the constant data rate requirement of each UEs, $R(SINR_u)$ is the data rate per PRB by user u , and N_{tot} is the total number of resources [18]-[20].

3.2. Algorithm Design

The actual traffic-based load-aware DPS is proposed in this work. The algorithm to reselect the serving cell proposed here is based on the criteria including CQI as well as the cell load condition of the potential TP(s). In the first step, each cell in the simulation scenario is calculated for the actual traffic load by using the equation (4). If the actual traffic load of each cell in eNBs is more than 80%, the targeted number of offloading UEs will be increased, otherwise decreasing the targeted number of offloading UEs. For those congested cells (set here with >80% cell load), UEs with low link quality are considered for changing of a serving cell. The new serving cell that provides the best connection can be chosen from the selection of cells within the CoMP cluster. The offloaded UEs' serving cells will be reselected in case of the offloaded cell has turned congested and the UE receives low link quality. The threshold for maximum cell load has also been set to make sure that offloaded cells have enough capacity to admit additional connections without affecting the currently attached UEs. The algorithm design of the proposed actual traffic base load-aware DPS is shown below.

Algorithm: Actual Traffic base Load-aware Dynamic Point Selection

```

//Initialization
j: Cell
J: Number of Cell
N: Number of offload UEs
M: Number of offloaded UEs

//Calculate actual traffic cell load
for j = 1 to J
    | Cellulate actual traffic cell load(j) by eq. (4)
end

//Calculate the number of offload UEs in each cell
Set N to zero
for j = 1 to J
    | if actual traffic cell load(j) > 80%
    | | Increase N(j)
    | else
    | | Decrease N(j)
    | end
end

//offload UEs
for j = 1 to J
    | if N(j) > 0
    | | Sorting cell-edge UEs
    | | Set M to zero
    | | while N < M
    | | | //offload cell edge UEs
    | | | Offload cell-edge UE (reselect cell eq. (2))
    | | | Increase M
    | | end
    | end
end
    
```

```

else
    | continue
end
end
    
```

4. Simulation Model and Simulation Scenarios

4.1. Simulation Model

The downlink system level simulation has been used in this work to observe the system performance of the LTE-Advanced system embedded with our proposed DPS mechanism, the actual traffic-based load-aware dynamic point selection. The simulator used here was adapted based on the Vienna LTE system level simulator [21]. The adapted model is used to evaluate the system performance under four different test scenarios. Table 2 presents the simulation parameters used in this work.

Table 2: Simulation parameters

Parameters	Value
Bandwidth	15 MHz
Carrie frequency	2.1 GHz
CoMP cluster	3-cell intra-site CoMP
UE speed	3.6 km/h
Antenna configuration	2x2, single pair of cross-pole antennas both at Tx and Rx
Propagation scenario	3GPP Macro Case1, 500 m inter-site distance
Traffic	Video streaming, Data rate 512 kbps
Scheduler	Proportional Fair (PF)
Handover interval	50 ms
Simulation Time	3,000 ms
Number of UEs	Normal load - uniformly distributed with 10 UEs/cell, Hotspot load - 50 UEs/cell

4.2. Simulation Scenarios

The 3-cell intra-site CoMP cluster as defined by 3GPP [3] has been used to define the coordinating area as a UE CoMP set, also known as the co-operating cluster. Figure 2 depicts the 3-cell intra-site CoMP cluster. In this work, this CoMP cluster is used as the COMP clustering pattern in the LTE-Advanced system studied here.

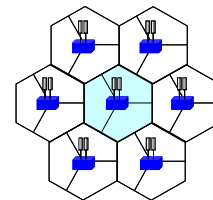


Figure 2: The 3-cell intra-site cluster

Four simulation scenarios have been implemented. Figure 3 shows the plot of UEs distribution within the Region of Interest (RoI) with regards to each simulation scenario. Base on the 3-cell intrasite CoMP cluster, as shown in Figure 2, the test scenarios

were designed in such a way that the system performance under heavy traffic as well as the hotspot type of traffic distribution can be observed. The four simulation scenarios implemented here consists of the randomly and uniformly distributed UEs (with normal traffic load) in scenario 1 and the hotspot scenarios with different hotspots' locations (high load in certain areas) in scenario 2 - 4. There are 19 eNBs or 57 cell sites in the simulation scenario. The red dots in Figure 6 represent the eNB and the blue crosses represent the position of the UEs.

In the first simulation scenario, 10 UEs are uniformly distributed within each cell to mimic the system under normal traffic load as illustrates in Figure 3(a). In the second scenario, one cell in each CoMP cluster (under the coverage of each eNBs) has 50 UEs located in to form a hotspot and 10 UEs on the other cells in the same cluster, as shown in Figure 3(b). There are three scattered hotspots implemented in simulation scenario 3 and 4. In scenario 3, the hotspot cells generated with 50 UEs are in the exact location of the three cells of one eNB. In other words, 150 UEs were located in those eNBs for high traffic demand areas, as illustrated in Figure 3(c). The last simulation scenario is similar to that presented in scenario 3. However, each three 3-cell coverage hotspot was located across three different clusters as can be seen in the Figure 3(d).

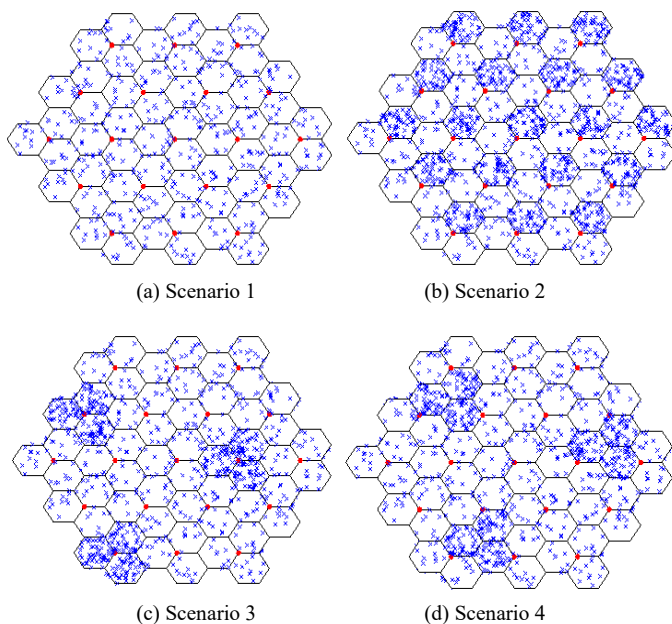


Figure 3: The plot of UEs distribution in the different scenario

5. Simulation Results

In this section, the simulation results obtained from the adapted system level simulator discussed in section 4 are presented. For the comparative studies, different mechanisms have been configured to observe the system performance including the non-DPS system (traditional LTE Advanced system), DPS (with received signal strength-based), and our proposed DPS with load-aware using actual eNBs' real-time traffic situation. The observed results for system performance evaluation include 1) the throughput performance i.e. the peak

throughput, the average throughput, and the cell-edge throughput 2) The number of UEs achieving the expected data rate and 3) eNBs' traffic load.

5.1. Peak, Mean, Edge Throughput Performance

Figure 4 – 7 illustrate the simulation results of the test scenario 1 – 4, respectively. The x-axis identifies different types of throughput observed from the simulation including the peak throughput, the mean throughput, and the cell-edge throughput. The y-axis represents the throughput level in Mbps. Different colored bars represent the throughput performance obtained from a non-DPS system (in blue), a system embedded with a traditional DPS mechanism (in orange), and a system embedded with our proposed DPS mechanism (in gray).

The simulation results for test scenario 1 are given in Figure 4. It can be seen that when the system operated under normal traffic load, the system performance in terms of peak throughput, average throughput, and cell-edge throughput provided by implementing the three mechanisms i.e. non-DPS, DPS, and DPS with actual traffic load-aware are the same. This is because with a low number of UEs, traffic demand from the generated UEs is low. Hence, the system is not saturated and has no problem providing good Quality of Service (QoS). As a result, the system embedded with three different mechanisms offer similar performance.

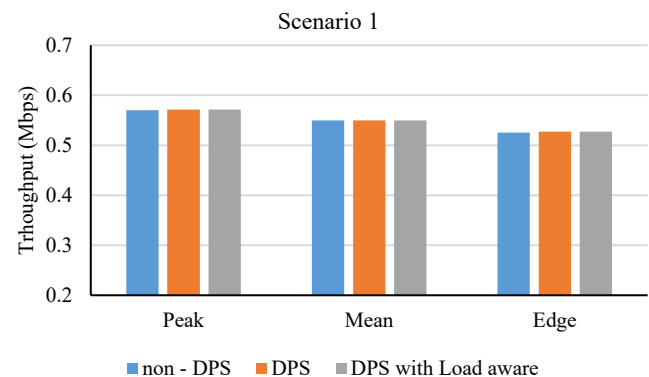


Figure 4: Simulation results from scenario 1

Figure 5 shows the simulation results obtained via test scenario 2. It can be seen that in the case of non-DPS and typical DPS mechanisms, the system performance is similar though slightly higher peak, mean and edge through are offered by the DPS mechanisms. When comparing DPS with load-aware DPS, it is obvious that the throughput performance offered by our load-aware DPS is the highest for peak, mean, and edge. Since in scenario 2, the hotspot is located in one of the three cells in each cluster. In other words, there is a load imbalance among the cells in the same cluster. As a result, traffic can be offloaded from the congested cell to the neighbor(s) (within the same cluster) who handle a small number of UEs. With the load-aware mechanism, the overall system can then be highly improved.

Figure 6 and Figure 7 present the simulated results of the test scenario 3 and 4, respectively. The hotspot cells were allocated with the same number of UEs. However, the positions of hotspot cells are at different locations. In test scenario 3, it can be seen

from the simulation results that system performance obtained using the three mechanisms provides similar results. As in this scenario, although there are hotspot areas with highly generated traffic demand, the high traffic load covers the entire CoMP clusters, which makes it rather impossible to transfer the heavy load to the cell(s) with lower traffic. This is due to the property of the fixed clustering mechanism.

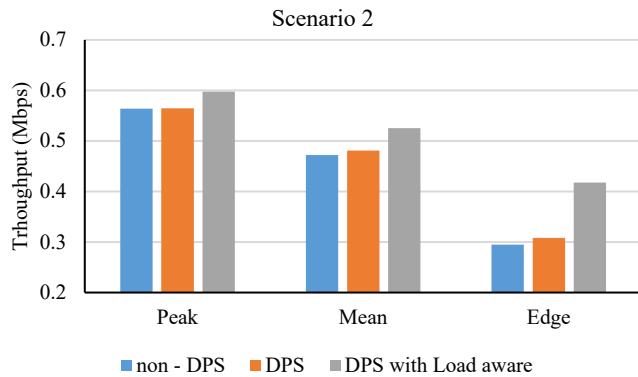


Figure 5: Simulation results from scenario 2

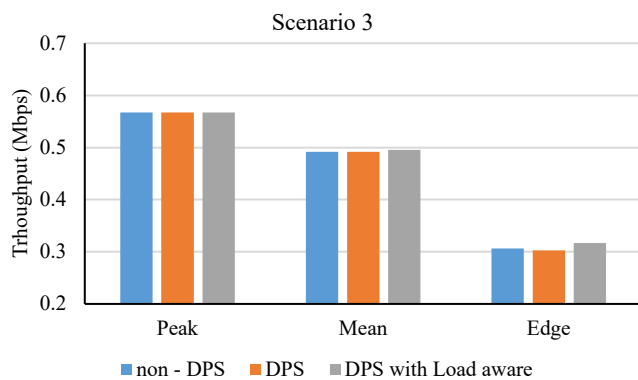


Figure 6: Simulation results from scenario 3

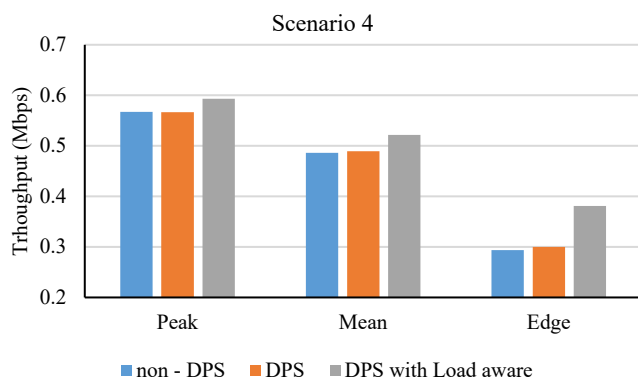


Figure 7: Simulation results from scenario 4

Simulation scenario 4 observes the case when the hotspots' coverages are across the fixed CoMP clusters. From the simulation results, shown in Figure 7, it can be seen that although it has the same number of UEs as in scenario 3, the DPS mechanism offers slightly better throughput performance in general. But When the actual traffic load of eNBs is considered as

the main part of the offloading condition, our DPS with a load-aware mechanism provides much better results, especially for the cell edge throughput. It can also be seen that the results from scenario 2 and 4 are very similar, which is due to the ability of the proposed load-aware DPS mechanism in such a way that higher loaded cell can offload some UEs to those with available resources, thereby allowing better overall system performance and capacity.

5.2. The Number of UEs Achieving Expected Data Rate

In this section, the results are presented in the view of users' experience. Note that the video streaming traffic model has been implemented here to mimic the realistic use cases. Figure 8 shows the results for the number of UEs (as in percentage) that achieve the expected data rate (512 kbps) for all test scenarios. The results provide a comparison for the system embedded with non-DPS, DPS, and our DPS with actual traffic load-aware, represented by the blue bars, the orange bars, and the gray bars, consequently.

In simulation scenario 1, all UEs achieve the expected data rate (100%) for all three mechanisms. With low traffic demand, all three systems can maintain system performance. In scenario 2, it can be seen that in the case of the non-DPS mechanism, only 50.3% of UEs can achieve the expected data rate, while the DPS mechanism offers 3.4% higher. Using DPS with load-aware mechanism, the number of UEs achieving expected data rate increases by 16.3% to 66.9% satisfying users. Note that, in this scenario, one-third of the entire simulation plane has high traffic demand. In scenario 3, the number of UEs that can gain the expected data rate is approximately 63% for all DPS mechanisms. It can be concluded that in the event of a hotspot occurring in all cells of the CoMP cluster, no matter what DPS mechanism is used, the system performance cannot be further enhanced as the hotspot cells have entered the saturated stage.

The different situation can be seen from the results of simulation scenario 4. DPS mechanism provides the number of UEs achieving expected data rate at approximately 61%, which is rather close to that of the non-DPS mechanism. On the other hand, when the proposed DPS with actual traffic load-aware is used, the number of UEs achieving the expected data rate increases by approximately 9% to the 70.4% of all users. This is due to the real-time awareness of actual traffic, which each cell is handling, by using our proposed mechanism. As a result, unsatisfying UEs, who are most likely located at the cell edge of the hotspot cells (saturated cell) can be offloaded to the cell in the same CoMP cluster with more available resources (lower traffic).

Coined from the comparison, in the event that the number of UEs in each cell is small, the system is not saturated, thus all UEs can achieve expected data rate. In the case that the number of UEs in some cells of the CoMP cluster is high (saturated traffic), when using the proposed DPS mechanism with load-aware, traffic load can be transferred to other cells in the same CoMP cluster with more availability to handle the new connections, thus increasing the number of UEs achieving the expected data rate. On the other

hand, in case of all cells in a CoMP cluster becoming hotspot or has a high number of UEs, the use of DPS and DPS with load-aware mechanisms only cannot increase the number of users achieving the expected data rate. This leads to the plan for our future work to consider also the clustering mechanism in combination with our proposed DPS mechanism to further enhance the system performance through best resource utilization.

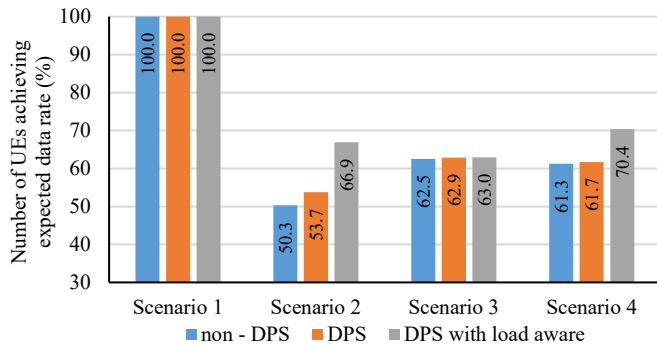


Figure 8: Number of UEs achieving expected data rate

5.3. Offered Traffic Load

Figure. 9 - 11 illustrate the traffic load of each cell (sector) in a CoMP cluster obtained from the scenario 2. Refer to Figure 3(b), each CoMP cluster is generated with one hotspot cell and the other two normal-traffic cells, known as intra-site CoMP cluster. It can be seen that cells with a large number of UEs or hotspot cells are handling a lot of traffic, no matter what mechanism is being used, since the system has been saturated, as shown in the plot of offered traffic in Figure 9.

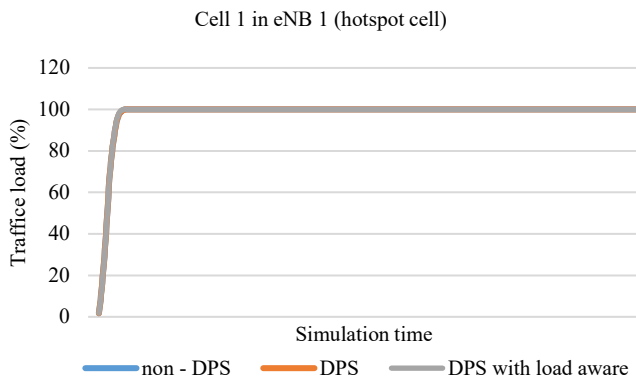


Figure 9: Traffic load of cell 1 in eNB 1 (hotspot cell), scenario 2

Figure 10 and 11 show the traffic loads of cell 2 and 3 in the same CoMP cluster as cell 1. In the case of the non-DPS mechanism, these cells with a low number of generated UEs has offered traffic at approximately 20%, but when using the DPS mechanism, traffic load are slightly higher. In the case of the DPS with a load-aware mechanism, traffic load increases to around 35% and 50% in cell 2 and cell 3, respectively. This set of results confirm that our DPS with load-aware mechanism checks the actual traffic load of every cell in the CoMP cluster and uses that as one major criterion for dynamically selecting the transmission point at each decision-making interval. Hence, when one cell is

saturated, the load will be transferred to the other cell(s) in the same CoMP cluster. As seen in the results, the traffic load of cell 1 is offloaded to cell 2 and cell 3. The amount of offloading traffic is not necessarily the same for each cell. It depends on how close the UEs to the cell-edge and the level of traffic loads of the offloading and offloaded cells. Hence, the traffic load results of DPS with the load-aware mechanism shown in Figure 10 and 11 are not the same.

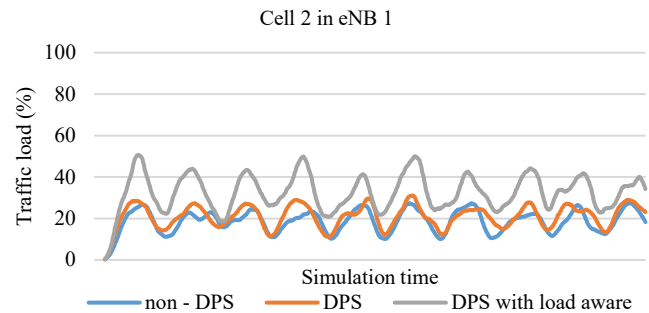


Figure 10: Traffic load of cell 2 in eNB 1, scenario 2

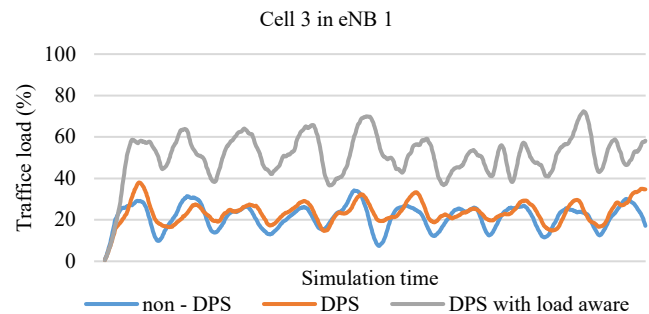


Figure 11: Traffic load of cell 3 in eNB 1, scenario 2

6. Conclusion

In this paper, the actual traffic load-aware DPS has been proposed. The system performance of the traditional LTE-Advanced system, the system embedded with baseline DPS mechanism, and the system embedded with our proposed DPS with actual traffic based load-aware mechanism are investigated. The adapted Vienna downlink system level simulator has been used for the system evaluation. The video streaming traffic model adapted here has been deployed with a data rate of 512 kbps for realistic use cases. The system performance is observed in different dimensions including the throughput performance (peak throughput, mean throughput, and cell-edge throughput), the number of UEs achieving expected data rate, and the traffic load illustrated for each cell in the imbalanced offered traffic scenarios, i.e. simulation scenario 2 implemented here. The four different scenarios have been investigated covering uniformly distributed traffic over the simulation terrain as well as different patterns of hotspot cases. While in the non-saturated traffic case and congestion covering the entire cluster case, all mechanisms perform similarly, our proposed mechanism offers a significant system performance improvement over the other DPS mechanism and traditional system for cases with irregular or imbalanced traffic within a CoMP cluster. As for our future work, a more

flexible clustering mechanism will be studied to further enhance our mechanism.

Conflict of Interest

The authors declare no conflict of interest.

References

- [1] Cisco, "Cisco Visual Networking Index: Global Mobile Data Traffic Forecast Update, 2016-2021," 2017.
- [2] N. Teerasuttakorn, K. Nuanyai, A. Zamani, A. Schmeink and S. Chantaraskul, "Study of Almost Blank Subframe Configurations for Traffic offload in HetNets," 2018 International Conference on Information and Communication Technology Convergence (ICTC), Jeju, 2018, 201-206, doi: 10.1109/ICTC.2018.8539494.
- [3] 3GPP The Mobile Broadband Standard (2012). Release 11, from https://www.3gpp.org/ftp/Information/WORK_PLAN/Description_Release_s/Rel-11_description_20140924.zip
- [4] M. Elhattab, M. -A. Arfaoui and C. Assi, "CoMP Transmission in Downlink NOMA-Based Heterogeneous Cloud Radio Access Networks," in IEEE Transactions on Communications, **68**(12), 7779-7794, Dec. 2020, doi: 10.1109/TCOMM.2020.3021145.
- [5] J. Chen, X. Ge, Y. Zhong and Y. Li, "A Novel JT-CoMP Scheme in 5G Fractal Small Cell Networks," 2019 IEEE Wireless Communications and Networking Conference (WCNC), Marrakesh, Morocco, 2019, 1-7, doi: 10.1109/WCNC.2019.8886024.
- [6] A. Marotta, D. Cassioli, C. Antonelli, K. Kondepu and L. Valcarenghi, "Network Solutions for CoMP Coordinated Scheduling," in IEEE Access, **7**, 176624-176633, 2019, doi: 10.1109/ACCESS.2019.2957940.
- [7] K. Nuanyai and S. Chantaraskul, "Study of TP Switching Period and SINR Margin in Dynamic Point Selection for LTE-Advanced," 2019 7th International Electrical Engineering Congress (iEECON), Hua Hin, Thailand, 2019, 1-4, doi: 10.1109/iEECON45304.2019.8938876.
- [8] Y. Gao, Y. Li, H. Yu and S. Gao, "Performance analysis of dynamic CoMP cell selection in LTE-advanced Heterogeneous Networks scenario," 2011 International Conference on Uncertainty Reasoning and Knowledge Engineering, Bali, 2011, 173-176, doi: 10.1109/URKE.2011.6007937.
- [9] K. Michail et al., "A load and channel aware dynamic point selection algorithm for LTE-A CoMP networks," 2016 International Conference on Telecommunications and Multimedia (TEMU), Heraklion, 2016, 1-5, doi: 10.1109/TEMU.2016.7551928.
- [10] R. Gupta, S. Kalyanasundaram and B. Natarajan, "Dynamic Point Selection Schemes for LTE-A Networks with Load Imbalance," 2015 IEEE 82nd Vehicular Technology Conference (VTC2015-Fall), Boston, MA, 2015, 1-5, doi: 10.1109/VTCFall.2015.7390905.
- [11] R. Agrawal, A. Bedekar, R. Gupta, S. Kalyanasundaram, H. Kroener and B. Natarajan, "Dynamic point selection for LTE-advanced: Algorithms and performance," 2014 IEEE Wireless Communications and Networking Conference (WCNC), Istanbul, 2014, 1392-1397, doi: 10.1109/WCNC.2014.6952393.
- [12] Ali, Md. Shipon. "On the Evolution of Coordinated Multi-Point (CoMP) Transmission in LTE-Advanced," International Journal of Future Generation Communication and Networking, **7**, 91-102, (2014), doi: 10.14257/ijfgen.2014.7.4.09.
- [13] S. Singh, A. Kumar, D. S. Khurmi and T. Singh, "Coordinated Multipoint (CoMP) Reception and Transmission for LTE-Advanced/4G," International Journal of Computer Science and Technology, **3**(2), 212-217, April-June 2012. DOI: 10.14257/ijfgen.2014.7.4.09
- [14] A. S. Ahmad, M. J. Huque and M. F. Hossain, "A novel CoMP transmission mechanism for the downlink of LTE-A cellular networks," 2016 5th International Conference on Informatics, Electronics and Vision (ICIEV), Dhaka, 2016, 875-880, doi: 10.1109/ICIEV.2016.7760126.
- [15] C. Chae, S. Kim and R. W. Heath, "Network Coordinated Beamforming for Cell-Boundary Users: Linear and Nonlinear Approaches," in IEEE Journal of Selected Topics in Signal Processing, **3**(6), 1094-1105, Dec. 2009, doi: 10.1109/JSTSP.2009.2035857.
- [16] 3g4g.blogspot.com, from https://2.bp.blogspot.com/-R9Trs5R0o4/TYY-JGsNSh/AAAAAAAAADfk/_zcOHgcjVE/s1600/CoMP_NTTDocomo_2.jpg
- [17] G. Morozov, A. Davydov and I. Bolotin, "Performance evaluation of dynamic point selection CoMP scheme in heterogeneous networks with FTP traffic model," 2012 IV International Congress on Ultra Modern Telecommunications and Control Systems, St. Petersburg, 2012, 922-926, doi: 10.1109/ICUMT.2012.6459792.
- [18] I. Siomina and D. Yuan, "Analysis of Cell Load Coupling for LTE Network Planning and Optimization," in IEEE Transactions on Wireless Communications, **11**(6), 2287-2297, June 2012, doi: 10.1109/TWC.2012.051512.111532.
- [19] J. G. Andrews, F. Baccelli and R. K. Ganti, "A Tractable Approach to Coverage and Rate in Cellular Networks," in IEEE Transactions on Communications, **59**(11), 3122-3134, November 2011, doi: 10.1109/TCOMM.2011.100411.100541.
- [20] I. Viering, M. Döttling and A. Lobinger, "A Mathematical Perspective of Self-Optimizing Wireless Networks," 2009 IEEE International Conference on Communications, Dresden, 2009, 1-6, doi: 10.1109/ICC.2009.5198628.
- [21] M. Rupp, S. Schwarz and M. Taranetz, "The Vienna LTE-Advanced Simulators: Up and Downlink, Link and System Level Simulation," 11., Springer Singapore, 2016. DOI: 10.1007/978-981-10-0617-3.